



---

## **Monitoring and Prediction of Land Use/Land Cover Change using the Integration of Markov Chain Model and Cellular Automation in the Southeastern Tertiary Hilly Area of Bangladesh**

Sanjoy Roy <sup>a\*</sup>, Kaniz Farzana <sup>b</sup>, Mossammat Papia <sup>c</sup>, Mehedi Hasan <sup>d</sup>

<sup>a</sup> *Department of Geography and Environment, University of Dhaka, Dhaka 1205, Bangladesh*

<sup>b</sup> *Department of Geography and Environment, University of Dhaka, Dhaka 1205, Bangladesh*

<sup>c</sup> *Department of Geography and Environment, University of Dhaka, Dhaka 1205, Bangladesh*

<sup>d</sup> *Department of Geography and Environment, University of Dhaka, Dhaka 1205, Bangladesh*

<sup>a</sup> *Email: sanjoy87dhaka\_university@yahoo.com*

<sup>b</sup> *Email: shimnykaniz@gmail.com*

<sup>c</sup> *Email: papia\_papia86@yahoo.com*

<sup>d</sup> *Email: mehedi.sagor84@gmail.com*

### **Abstract**

Optical satellite imagery has been used for analyzing the spatial distribution; temporal changes and prediction of land use/land cover (LULC) categories in the southeastern hill tracts of Bangladesh. This is the primary work in this study area where multi-temporal Landsat imagery has been used to generate LULC maps for the years of 1989, 2003 and 2014. In the first step, a total seven LULC categories were derived using the integration of NDVI and conventional supervise classification techniques which were further evaluated using the error matrix table and kappa statistics. The result obtained from the accuracy assessment process presented an overall accuracy of more than 90% for all three years with Kappa statistics 1989 (88.67), 2000 (92.33) and 2014 (89.67) respectively.

---

\* Corresponding author.

A rigorous change analysis was carried out, using Land Change Modeler (LCM) where dramatic changes were noticed in hilly forest, shrub land and crop land categories for 1989-2014 time span. From 1989 to 2014 hilly forest decreased 3062 sq. km, shrub land and cropland increased 2990.82 sq.km and 258.74 sq.km area respectively. In the second stage, Markov chain-cellular automata was used to model and predict LULC in the study area. At first Markov chain was used to generate transition probability matrices between LULC categories and then cellular automata was used to predict 2014 LULC map. After successful validation of observed and predicted LULC maps of 2014 (Overall accuracy 91.43% and Kappa statistics 90.00), the combined procedure was employed to simulate land-use/land-cover for 2028 and 2042. The simulated result of 2014-2042 shown a dramatic decrease in hilly forest (1831 sq.km.) and water reservoirs (148 sq.km.) whereas a significant increase was noticed in the shrub land (1889 sq.km.), crop land (91 sq.km.) and settlement area (7.5 sq.km). All these findings from the research could offer an opportunity for the more skillful management and policy making on biodiversity, forest, land and other environmental resources in the study region.

**Keywords:** LULC; GIS; CHT; Markov; CA-Markov; LCM

## **1. Introduction**

Large scale modification of Earth's surface has been intensifying worldwide due to the rapid increasing of anthropogenic activities [27] in response to industrialization and urbanization which has significant impact on earth's physical, biological and human environments. Among those, one of the apparent modification of earth's surface induced by human being is the land use/cover change which has though been happening from the very outset of civilization but in recent times it has outbursts worldwide. This could be defined as a silent disaster for terrestrial ecosystem which directly affects the degradation of soil [23, 43] through accelerating erosion of the most nutrient rich top soil, breaking food chain, damaging wildlife habitats and thus immense loss of biodiversity [46, 17] and ecosystem services [36]. This has also been added pollution to the atmosphere, hydrosphere and biosphere from various points and non-point sources [45], increased concentration of CO<sub>2</sub> and other greenhouse gases in the atmosphere [18], disrupted the hydrological cycle and so on. In hilly area major changes occurred due to shifting cultivation on hill slopes, clearing of hilly forest and cutting and converting of hills to the plain land for settlement and other establishments. Therefore, the LULC changes from human existence have been increasing adverse impact on the global environmental systems which is sometimes irreversible for restoration.

Geographic Information System (GIS) and Remote Sensing (RS) have long been used and widely accepted as very powerful techniques in change analysis and simulation of LULC. Combined, they are capable of critical analysis and decision supports in earth's surface changes within shortest time with reasonable accuracy. RS is applied to retrieve information from analysis of earth observatory multi-temporal and multispectral satellite images of different spatial resolutions. These images offer tremendous opportunity in LULC monitoring [30] including historical trends and future simulation which are undoubtedly necessary in the sustainable land use, planning and policy making for both governmental and non-governmental level. Information's obtained from remotely sensed data are further used in GIS to perform modeling and simulation of LULC [31, 32]. There are basically two categories of LULC models, of which one is spatial and other is aspatial category [42].

A spatial models are used to quantify predicted LULC in a particular region and associated driving forces [42] whereas empirical-statistical models and rule based models included in the spatial category are mainly used in the analysis of LULC changing pattern and spatial location of existing and future potential changes. Among all spatial models the Markov chain model integrated with Cellular Automata has been widely used for spatio-temporal modeling of LULC in a reasonable way.

Bangladesh is a most densely populated deltaic country in the world with tertiary hills running from south east to the north along the eastern and north-eastern border and funneled shape Bay of Bengal to the south. The southeastern hilly part is commonly known as the Chittagong Hill tract (CHT) which administratively includes three hilly districts like Bandarban, Rangamati and Khagrachari. Major economic activities in this region are tourism industry, small scale trade, transport and agriculture sectors which put a great contribution to the national GDP of the country. According to the "CHTDF integrated Local Economic Development (LED) and Community Economic Empowerment (CEP) Strategy 2010-13" forestry shares 10% of the CHT GDP which is five times the national share (2%). Besides, agriculture, Trade and industry share 19%, 26% and 5% respectively. But in the last few decades rapid increasing of population (974,445 in the 1991; 1,331,966 in the 2001; and 1,598,231 in the 2011) (BBS, 1991, 2001, 2011) has been intensifying several environmental problems like; the damage of the ecology accompanied by loss of indigenous trees and crops, deforestation, degradation of soil quality by slash and burn agriculture (shifting cultivation) and thus changing LULC at large scale. Some research has been revealed that on average eight hectares of land is necessary to sustain for a household in the CHT. But existing shifting cultivation is not sufficient to meet the needs of the present population. Right now it requires adequate non-farming employment opportunities for their sustenance. Although its regret that there is limited or no scope for creating non-farming opportunities in the near future under existing policy. Thus, serious environmental degradation induced by continuous LULC changes is not so far. It is, therefore, imperative to take proper strategy and policy for sustainable land use plan in CHT to enable people for their secure and sustainable livelihood.

Hence, the main objective of this research is to map and monitor LULC changes from 1989 to 2014 in response to increasing anthropogenic pressure from over exploitation of natural resources and also to simulate the future scenario, if the current trend of conversion is continued by using spatial modeling (Markov chain and cellular automata).

## **2. Materials and Methods**

### **2.1. Study area**

With an area of 5089 sq. miles (13295 sq. km.) the Chittagong Hill Tract (CHT) region is located in the southeastern part of Bangladesh between 21°25' N to 23°45' N latitude and 91°45' E to 92°50' E longitude. The region is surrounded by the Indian state of Tripura to the north, and Mizoram to the east, Myanmar to the southeast, Chittagong district to the west and Cox's bazar district to the southwest. It is a part of Hill Tripura and Arakan Yoma branching off from the Himalayan range and Continuing to the south through Assam and Hill Tripura of India to Arakan of Myanmar [38, 40].

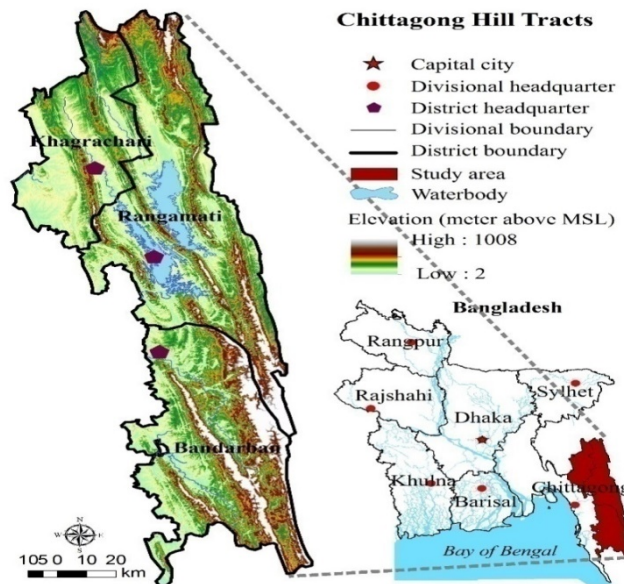


**Figure 1:** Location setting of the study area.

The CHT is the single extensive hilly region of the country which uplifted during the tertiary period of geological time scale. It consists of three hilly districts Rangamati, Khagrachari, and Bandarban which combined covers about 10% of the Bangladesh territory, but only 1% of the country's population [38] (Figure 1). The region is predominantly in mountainous topography whereas two-thirds of the region are characterized by steep slopes and the remaining area comprises of undulating topography [37]. The steep fold mountains in this region are aligned in a north-northwest to south-southeast which are composed of mainly weakly lifted sandstone, shale and some conglomerates [4]. The high hills along with parallel ridges with summits reaches nearly 300-1000 m above mean sea level [8].

The climate of the region is characterized by a tropical monsoon climate with mean annual rainfall is nearly 2540 mm in the north and east and 2540 mm to 3810 mm in the south and west [5]. Approximately 80% rainfall occurs during the period of May to September. The mean monthly maximum temperature of this region is 25°C to 34°C [2, 19]. The vegetation is characterized by semi-evergreen deciduous to tropical evergreen rain forest dominated by tall trees and grasses [5]. This region is enriched with several natural resources like forestry, biodiversity, water, etc. It supports almost 80% of the country's total biodiversity [34] and the main source of bamboo of the country according to Ministry of Chittagong Hill tracts of Bangladesh. Geographically and culturally the region is distinct from the rest of the country.

The entire region is a home of 12 different indigenous ethnic groups known as "Tribes". According to the population census 1991, the total population in the hill tracts of Bangladesh was 974,447 of which 501,114 were tribal peoples with distinctive cultures. Total population enumerated in the 2011 census was 15, 87,000 out of which 50% people were tribes. The majority of these people depend on traditional agriculture, clearing land through slash and burn practice which is known as Shifting cultivation locally as Jhoom cultivation. During the recent years, this region underwent several environmental degradation due primarily to shifting cultivation, illegal commercial logging, especially on steep slopes, erosion of top soil etc.

**2.2. Data acquisition**

The use of satellite imagery has shown immense potential in the study and analysis of LULC in both regional and global scales. In this research Landsat data were used to find out the scenario of LULC changing pattern and their future extent throughout the CHT. The study area lies in two different paths and rows of Landsat image tile (path 135, 136 and row 44, 45). To cover the whole study area, 4 satellite scenes set for each year were obtained from the Earth Resources Observation and Science (EROS) Center through the USGS Global Visualization Viewer and thus 12 cloud-free images (four Landsat5-TM images for 1989, four Landsat7-ETM+ images for 2000 and four Landsat8-OLI for 2014) were acquired for the dry season (December- January) in order to minimize seasonal influences (Table 1). Apart from satellite imagery a number of referenced dataset including topographic map (1: 50,000 scale), contemporary high resolution satellite imagery (World View-2 image of 2000; GEOEYE-1 image of 2013; Google Earth image of 2014) and ancillary secondary maps were acquired for accuracy assessment of the classification. A total 600 ground truth points were collected using a high resolution handled GPS (Garmin GPSMAP 62s) directly from field survey during 2013-2014 to assist in the accuracy assessment process.

**Table 1:** Image information used in the study.

SL. No.	Sensor	Date of acquisition	Year	Path	Row
1	Landsat TM4	21st January	1989	136	44
2		21st January		136	45
3		14th January		135	44
4		14th January		135	45
5	Landsat7 ETM+	21st December	2000	136	44
6		21st December		136	45
7		12th November		135	44
8		12th November		135	45
9	Landsat8 OLI-TIRS	2nd January	2014	136	44
10		2nd January		136	45
11		11th January		135	44
12		11th January		135	45

**2.3. Geometric correction**

All satellite images acquired from the EROS data center were already geometrically corrected, followed by the global geographic coordinate system (WGS 1984) and further geo-rectifications of all four images of 1989 were accomplished using a total 80 ground control points (GCPs) taken from topographic map of 1990. Projection system was set to Bangladesh Transverse Mercator (BTM), a country-specific UTM projection system developed by WRPO (Bangladesh Water Resource and Planning Organization) in 1996.

A 1<sup>st</sup> order polynomial fit was used and the images were re-sampled to 30 meter pixel size using the nearest

neighbor re-sampling technique. Based on 1989 geo-rectified images, all other images of 2000 and 2014 were co-registered to the desired projection system and pixel size following the above mentioned re-sampling technique with root mean square error (RMSE) of less than 0.5 pixel, which indicating a satisfactory level for image comparison [22, 44]. While doing this we identified the pixels (total 80) of same permanent features (buildings and road edges) in both images to co-register them.

#### **2.4. Image preprocessing**

As the images were taken from different months of the year based on availability of cloud free data, they might be influenced by seasonal disturbances and atmospheric effects like aerosols, dust particles, cloud, varying sun angle etc. Besides, noises in data are also results from limitations in sensing by the sensor, signal digitization, or data recording process.

These noises from different sources significantly degrade the radiometric information of the image [28]. So, these images were subjected to a rigorous atmospheric and radiometric correction to reduce the influences of clouds, atmosphere and sun elevation angle. Several atmospheric correction methods have been established such as; empirical dark object subtraction (DOS) technique [11], modified DOS method [20], cosine estimation of atmospheric transmittance (COST) [10], moderate resolution atmospheric transmission (MODTRAN) model developed by the United States Air Force and the Spectral Science, ATmosphericCORrection (ATCOR) developed by German Aerospace Center (DLR) and the Fast Line-of-sight Atmospheric Analysis of Spectral Hypercubes (FLAASH) incorporated in ENVI software. In this research ATCOR module of ERDAS IMAGINE-2014 was used to carry out the atmospheric correction process. ATCOR has two modules like ATCOR 2 and ATCOR 3 whereas the first one is used when there is no available external atmospheric data for operating the correction procedure and the second one is used for correction imagery of rugged terrain surfaces with available robust terrain data [3].

We used ATCOR 2 workstation which runs based on moderate spectral resolution atmospheric transmittance (MODTRAN 4) code [6] and considers a homogeneous atmospheric thickness over the scene. A number of calibration parameters (image acquisition data, sensor type (TM/ETM/OLI), sensor specific edited calibration file, solar zenith angle, estimated elevation of the surface in kilometer from the mean sea level, estimated scene visibility, aerosol model = rural and solar region = tropical rural) were set before running the process. Basic information about the scene such as, Image acquisition data, time, Sun elevation angle, *the spectral radiance (L<sub>Min</sub>) scaled to the minimum quantized calibrated pixel value (QCalMin) in watt m<sup>-2</sup>sr<sup>-1</sup>μm<sup>-1</sup>* and the spectral radiance (L<sub>Max</sub>) scaled to the maximum quantized calibrated pixel value (QCalMax) in *wattm<sup>-2</sup>sr<sup>-1</sup>μm<sup>-1</sup>* are retrieved directly from image metadata file. After reducing atmospheric effects, ATCOR 2 converts the digital numbers (DNs) of each pixel of each scene to at sensor spectral radiance (L) in *mWcm<sup>-2</sup>sr<sup>-1</sup>μm<sup>-1</sup>* and finally to surface reflectance (ρ) using the following equations (1 and 2) [3]. The resultant scene's pixel contained reflectance value ranging from 0 to 1.

$$L = C_0 + C_1 \times DN \quad (1)$$

Where,  $L$  is the at sensor spectral radiance,  $C_0$  and  $C_1$  are radiometric calibration coefficients calculated from  $L_{Max}$  and  $L_{Min}$  for each spectral band and DN stands for the digital number of each pixel.

$$\rho = \frac{\pi(d^2L - L_{path})}{\tau E_g} \quad (2)$$

Where,  $d$  is the earth-sun distance in astronomical unit,  $\tau$  is the ground to sensor atmospheric transmittance,  $E_g$  is the global flux on the ground,  $L_{path}$  is the atmospheric path radiance caused mostly by the floating dust and aerosol,  $\pi = 3.1426$  and  $\rho$  is the surface reflectance.

Once atmospherically corrected, every image set containing four images of each year was mosaicked using seam line mosaicking method to prepare a single scene of each study year. Thus, 3 single scenes were generated which were further clipped to the boundary of the study area using an area of interest (AOI) derived from the vector file (ESRI shapefile) of the study area.

### 2.5. Image classification

The modified Anderson Level I classification Scheme [1] which is the worldwide accepted and widely used LULC classification scheme was used in this study to achieve desired LULC categories from satellite imagery.

**Table 2:** Classification scheme of LULC used in this study.

LULC Category	Description
Hilly forest	Evergreen and semi-evergreen forest covers, commercially planted forests with large canopy covers
Shrub land	Shrubs, bushes and scrub.
Crop land	Agricultural fields, Hill slope cultivated lands
Settlement area	Urban settlement, rural settlement, transportation network, commercial and industrial uses
River	Flowing water confined in a channel
Water reservoir	Perennial water body, lakes, ponds and other water reservoirs
Bare land	Open fields, exposed lands and sand fill areas

According to this classification scheme we identified 5 major classes as vegetation, settlement area, crop land, water body and bare land. For depth analysis, we again subdivided vegetation into hilly forest, shrub land and water body into the river, water reservoir respectively (Table 2). To generate the desired categories from the Landsat images we applied an integrated image classification method which involved decision making at each stage from the combination of both index-based and conventional classification-based approaches (Figure 2). Normalized difference vegetation index (NDVI) is a very common and widely used method to retrieve the vegetation information which uses the red and infrared band of satellite imagery [39].

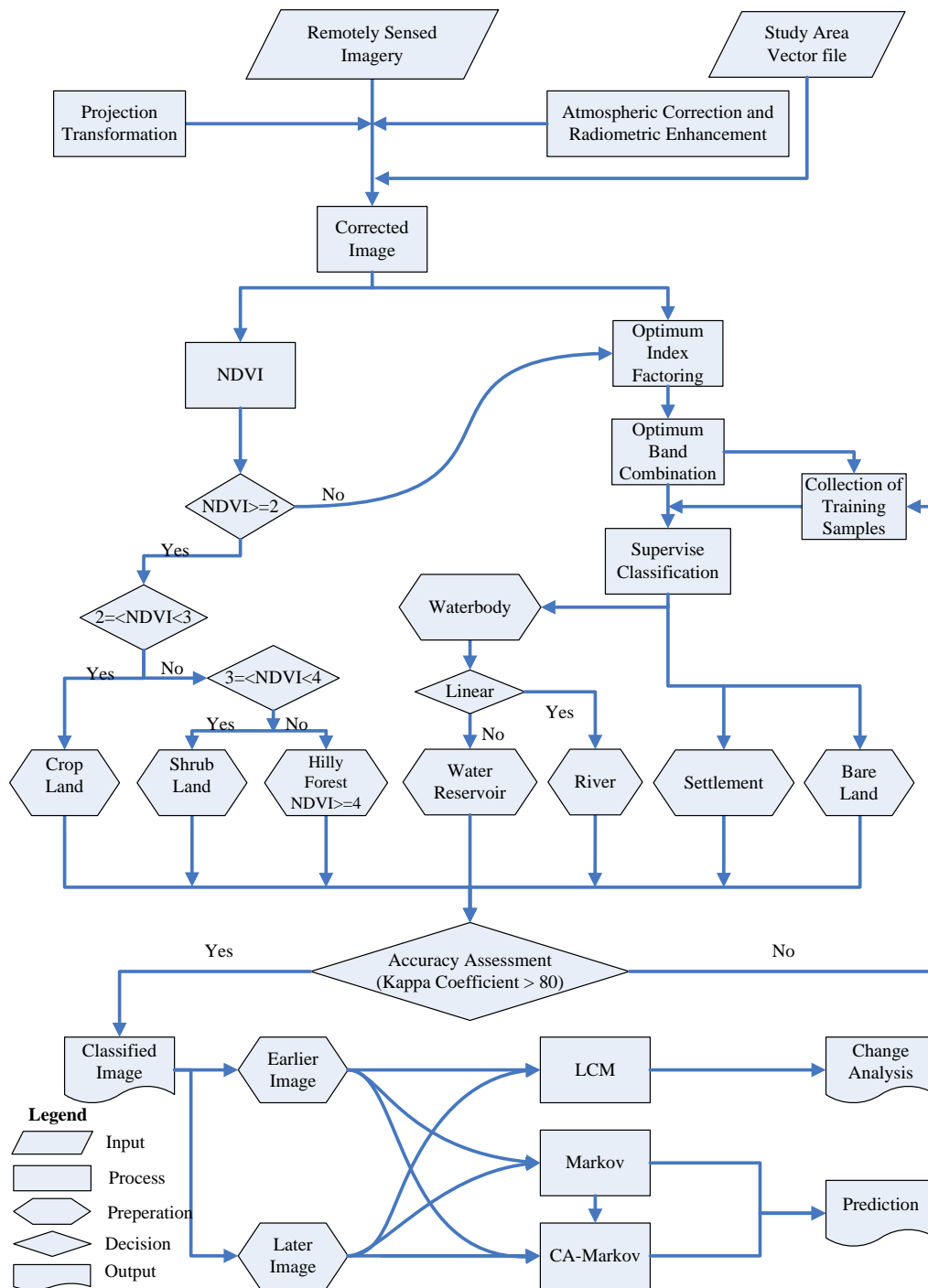


**Figure 2:** Work flow of the research.

We used different NDVI threshold values to efficiently retrieve crop land and forest covers as  $2 \leq NDVI < 3$  for crop land,  $3 \leq NDVI < 4$  for shrub land and  $NDVI \geq 4$  for the dense hilly forest. After retrieving the crop land and forest coverage classes we calculated an optimum index factor (OIF) [12] for the rest of the areas with a view to apply the Maximum Likelihood

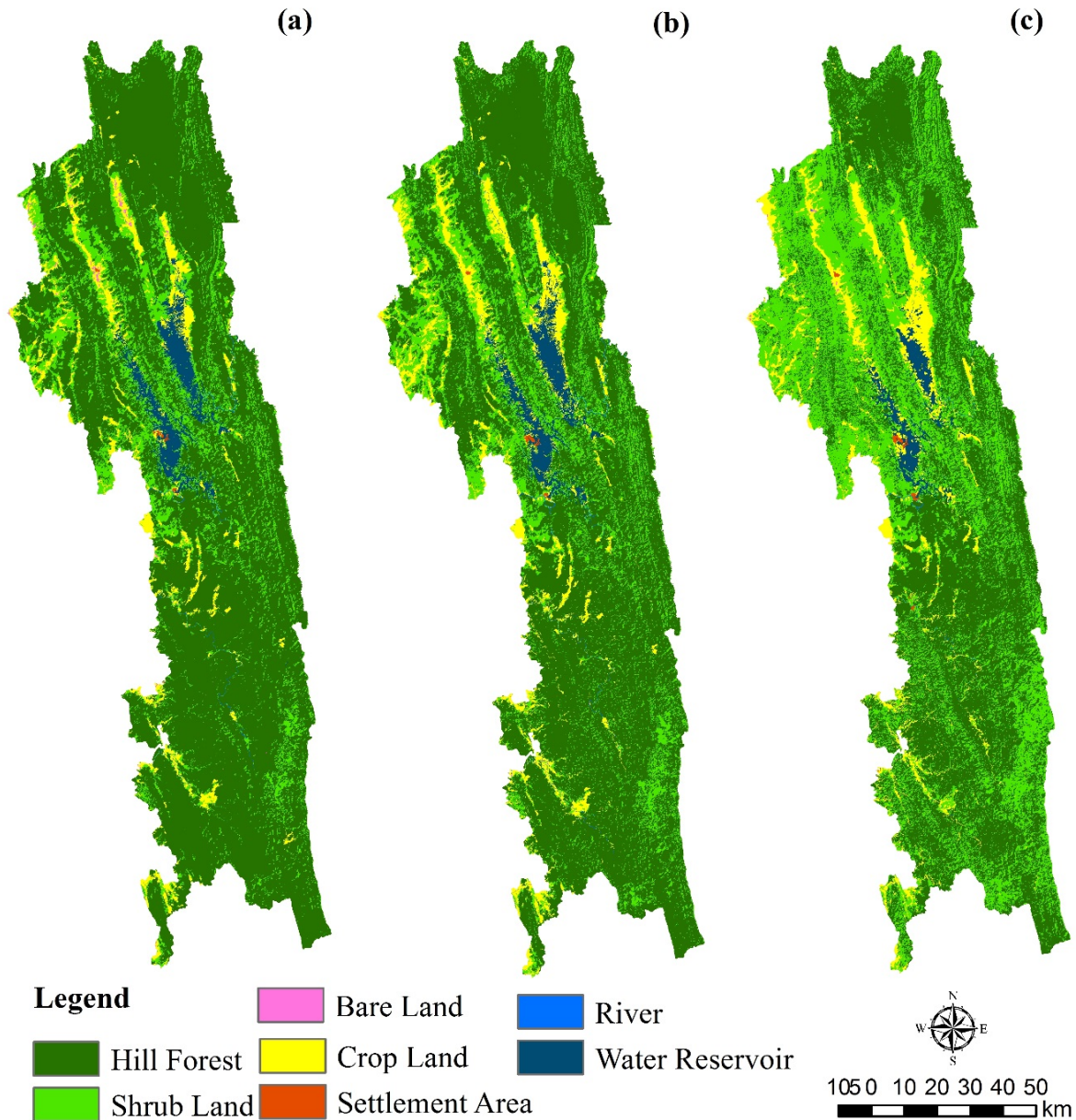


**Figure 3:** Existing LULC categories obtained from image classification. (a) 1989, (b) 2000, (c) 2014.

Supervised classification method. OIF was primarily employed to find out the optimum informative band composite image with minimum correlation among spectral bands from where training sites for classification could be compiled efficiently. Using those spectral bands, false color composite images were prepared for each study year. A total 200 signatures for each LULC class were extracted randomly covering the whole study area using the ERDAS Imagine software. Signatures were generated using the region growing technique of ERDAS Imagine that produces each region having similar spectral characteristic pixels based on the nearest neighborhood method. The maximum size of each region was set to 1000 pixels and the Euclidean spectral distance was set to 4 in digital number (DN) unit to accept pixels within this spectral distance from the digital number of the seed pixel. The signatures of each LULC class were evaluated examining the Transform Divergence (TD) values where the TD values for every class were obtained above 1900.

Based on these signatures a maximum likelihood supervised classification technique was used to classify the image into other desired classes such as settlement, water body and bare land. We further subdivided the water body into rivers and water reservoir based on the shape linearity. Linearity above 80% was classified as the river and others were classified as the water reservoir. Eventually, whole classes were stacked together and obtained the final LULC class of each year (Figure 3).

### **2.6. Post classification refinement and accuracy assessment**

The classification procedure left some misclassified or poorly classified pixels in each image which is commonly known as the salt and pepper effect [28]. It was happened mainly due to the similar spectral characteristics of some pixels in two different categories. Misclassification mainly happened along the boundary of crop land and shrub land. It was also happened in classifying rural settlement as mostly they are under the tree canopy. Some isolated pixels of different classes were found to be generated within the other classes. Therefore, a post classification refinement was desired to minimize misclassification. To minimize the number of isolated pixels, we applied a 3x3-pixel window mode filtering to assign the isolated pixels to the surrounding dominant class. Misclassification happened in the shrub land and crop land was further reduced using contemporary high resolution satellite image and secondary maps. In order to assess the accuracy of the classification it is essential to apply an accuracy assessment process.

Among the different accuracy assessment model the error matrix (confusion matrix or a contingency table) has become the most efficient method of reporting the accuracy of classification obtained from remotely sensed data [14] because the accuracy of each classified category (user accuracy and producer accuracy) is estimated along with the errors of inclusion (commission error), errors of exclusion (omission error) as well as an overall accuracy of the classification [15, 16]. Another estimator of accuracy is the Kappa statistics ( $K_{\text{hat}}$ ), which is a non-parametric discrete multivariate technique developed by Cohen [13] measures the overall agreement of a matrix. For the accuracy assessment, a total 350 sample pixels (50 per category) were generated using the stratified random sampling method over the study area for all three periods LULC maps.

An extensive field survey was conducted and a set of GEOEYE-1 pan-sharpened image-2013 were used to collect ground truth data for 2014, whereas high-resolution contemporary satellite imagery was used to collect ground truth data for 2000 map. Some other relevant maps collected from the Chittagong City Corporation were used in collecting ground data for the 1989 map. The classification accuracy assessment process was performed using the class values and the ground truth values and finally generated the error matrix containing different statistics of measurement (Table 3). A rigorous Kappa statistic for the stratified random sampling method was also used using the following equation (3) [7].

$$K = \frac{N \sum_{i=1}^r X_{ii} - \sum_{i=1}^r (x_{i+})(x_{+i})}{N^2 - \sum_{i=1}^r (x_{i+})(x_{+i})} \quad (3)$$

Where, r is the number of rows in the matrix,  $X_{ii}$  is the number of observations in row-i and column-i (the diagonal elements),  $x_{+i}$  and  $x_{i+}$  are the marginal totals of row-r and column-i, respectively, and N is the number of observations.

**Table 3:** Overall classification accuracy and Kappa statistics.

Year	LULC category	Producer accuracy (%)	User accuracy (%)	Overall accuracy (%)	$K_{\text{hat}}$ (%)
1989	Bare land	97.73	86	90.29	88.67
	Crop land	82.35	84		
	Hilly forest	86.79	92		
	River	100.00	96		
	Settlement	97.92	94		
	Shrub land	77.19	88		
	Water reservoir	93.88	92		
2000	Bare land	97.87	92	93.43	92.33
	Crop land	86.54	90		
	Hilly forest	95.92	94		
	River	97.96	96		
	Settlement	100.00	96		
	Shrub land	86.79	92		
	Water reservoir	90.38	94		
2014	Bare land	100.00	90	91.14	89.67
	Crop land	81.82	90		
	Hilly forest	88.46	92		
	River	100.00	94		
	Settlement	100.00	94		
	Shrub land	80.00	88		
	Water reservoir	91.84	90		

The overall accuracy for 1989, 2000 and 2014 maps was 90.29, 93.43 and 91.14%, respectively, whilst the Kappa statistics ( $K_{\text{hat}}$ ) was 88.67, 92.33 and 89.67 respectively (Table 3). The  $K_{\text{hat}}$  (>80) for the 3 maps of three different time frames indicate a high degree of accuracy [24, 29] with minimal error propagation in classification method.

### 2.7. Markov chain and CA- Markov for LULC modeling and prediction

Markov chain (MC) analysis has been widely used for ecological modeling [33, 9] which is a stochastic process that takes into account the past state to predict the future changing of variables over time. Because of its immense ability to quantify the rates and states of conversion among and between categories respectively, it has been equally used in the LULC change modeling. In this research a combination of MC and a hybrid cellular automata (CA-Markov) technique was applied to predict LULC for 2014, 2028 and 2042 using the IDRISI Selva software. It requires two LULC data sets of different time frames based on which the probabilities of transition between periods are obtained. The MC model generally uses the following formula (4) in the simulation process of LULC changes.

$$A_{(t+1)} = B_{ij} \times A_t; B_{ij} = \begin{bmatrix} B_{11} & B_{12} & \dots & B_{1n} \\ B_{21} & B_{22} & \dots & B_{2n} \\ \dots & \dots & \dots & \dots \\ B_{n1} & B_{n2} & \dots & B_{nn} \end{bmatrix} \quad (0 < B_{ij} < 1; \sum_{j=1}^n B_{ij} = 1; i = 1, 2, 3, \dots, n) \quad (4)$$

Where,  $A_{(t+1)}$  and  $A_t$  are LULC at t+1 and t period,  $B_{ij}$  is the transitional probability matrix.

The MCA produces a transitional probability matrix, a transitional area matrix and a set of conditional probability images (suitability images). The transitional probability matrix contains the probability of changing of each LULC category to every other category, whereas the transitional area matrix contains the number of pixels that are expected to be converted from one LULC category to other categories over a specific period of time. On the other hand, the output conditional probability images represent the probability of each LULC class to be found in each pixel over the time. In this research, we used 1989, 2000 and 2014 LULC class maps obtained from image classification to operate MC model. The MC provided two transition matrices by the cross tabulation of two LULC maps (1989 and 2000) and a set of suitability maps to primarily predict 2014 LULC map (Figure 10). In the suitability maps highest value represents the maximum suitability of an existing LULC class likely to change to another class. While doing this, 1989 and 2000 LULC maps were harmonized in order to match the same number of classes in both maps, the background value and the proportional error was set to 0 and 15% respectively.

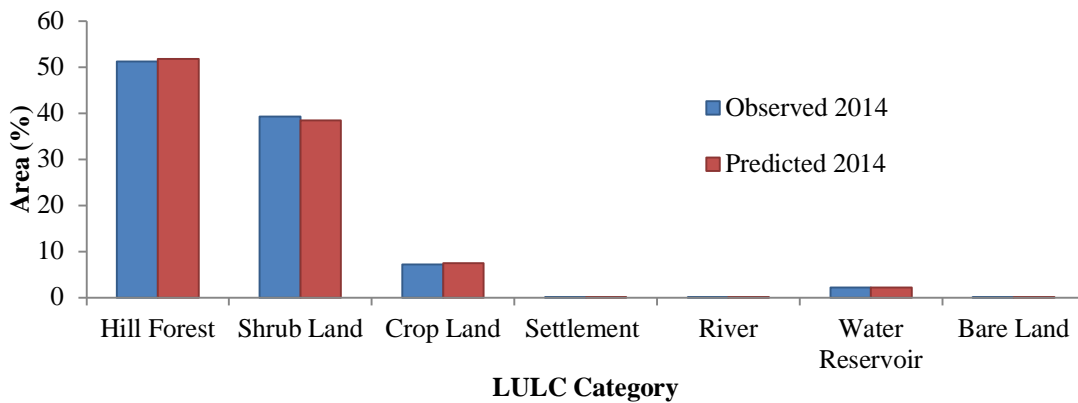


**Figure 4:** Area (%) of LULC category in observed and simulated maps.

As MC model doesn't itself provide the spatial location of future prediction of LULC, a hybrid CA-Markov was used to resolve this. CA-Markov is a combined Cellular automata, Markov chain, multi-criteria, and multi-objective land allocation model of LULC prediction process [41] where the projection is done based on the transition area matrix and suitability maps derived from the MC process. Firstly, we used 2000 LULC map as a base land cover data in CA-Markov module of IDRISI Selva-17 and cellular automata iterations was set to 14 (time lag between 2000 and 2014 is 14 years) in order to predict 2014 LULC map so that the simulated result could be compared with the existing LULC of 2014 to examine the model performance (Figure 4).

To predict 2014 LULC map the transition probability area matrix of 1989-2000, transition suitability maps and a 5\*5 kernel size standard contiguity filter (Figure 5) was used to ensure that the neighboring pixels were used to create spatially explicit contiguous weights to predict 2014 LULC map.

The accuracy of the simulation was assessed using the user accuracy, producer accuracy and overall accuracy statistics.

0	0	1	0	0
0	1	1	1	0
1	1	1	1	1
0	1	1	1	0
0	0	1	0	0

**Figure 5:** The 5\*5 standard contiguity filter.

In the producer accuracy assessment, crop land and shrub land categories shown comparatively poor simulation (72.58 and 79.37%) than other categories whilst in the user accuracy assessment all categories shown the result of more than 80%. This poor simulation of some categories is well addressed by many authors. According to Pontius and Malanson [35] the poor simulation of LULC categories may be the result of the nearness of existing LULC categories as CA-Markov uses the contiguity rule in the simulation process. However, the overall accuracy was 91.43%. Furthermore, we estimated the kappa coefficient to justify the agreement of simulation in response to the actual data. The  $K_{hat}$  (90.00) justified a reasonable agreement of the simulated result. Once successfully validated the simulated data with the actual data we went through the prediction for 2028 and 2042 LULC maps. In this stage we used 2014 LULC map as base data, transitional probability area matrix, transitional suitability maps, a 5\*5 kernel size contiguity filter and cellular automata iterations of 14 to simulate 2028 LULC map. As the same way 2042 LULC map was also simulated.

### 3. Results and Discussion

#### 3.1. Existing LULC scenario

Existing LULC classes by area for the year 1989, 2000 and 2010 are presented in (Figure 6). From the comparative analysis of LULC changing pattern, there was witnessing a significant divergence in the internal LULC categories. As a result, a huge change has been possible over the years through the conversion of one LULC category to others. For better understanding, we were able to detect gain, loss and net change for the three temporal periods: 1989-2000, 2000-2014, and overall 1989-2014 by LULC category (Figure 8).

To evaluate the results of land use/ cover conversion, a change area matrix was generated for the above time spans (Table 4). It shows the relational changing area of one LULC category to others over the delimited periods. From Figure 6 it is apparent that the entire study area is dominated by hilly forest and shrub land, whereas hilly forest covers the maximum extent of the area in all three study periods. As shown in the figure, major changes have been observed in hilly forest, shrub land and crop land. At a glance hilly forest has been continuously decreasing whereas continuous increasing have been observed in both shrub land and crop land categories. The most terrible scenario is the gradual declining of the inland water reservoirs which are the major sources of drinking water to the local indigenous community. These reservoirs also act as the sources of irrigation water in the dry seasons.

Besides, these are main fishing grounds of the hill tract and provide habitats for many water fowl bird species.

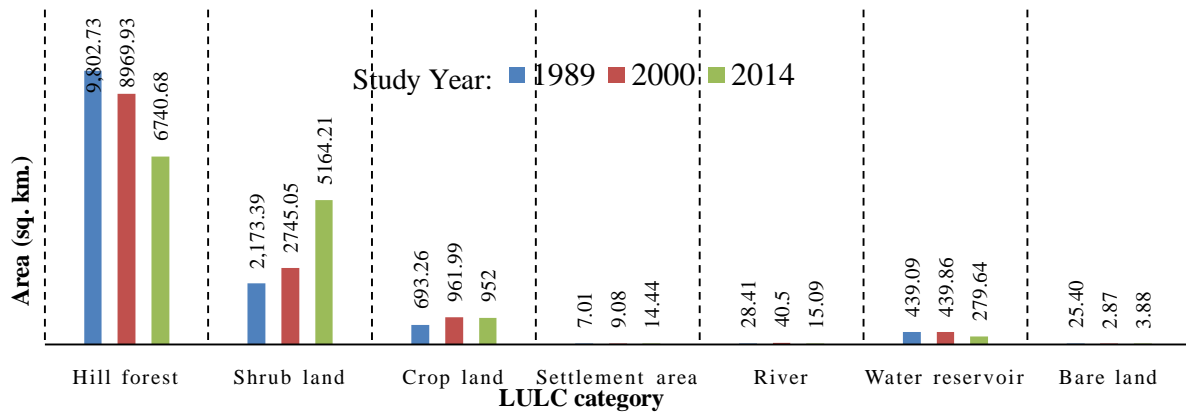


**Figure 6:** Existing LULC category by area.

### 3.1.1. Hilly forest

Hilly forest is the most dynamic LULC class in the study area. In 1989 it was the most extensive land cover in the study area, occupying 74.44% of the whole area (Figure 7) but it underwent several major changes over the time. In the following years a significant change has been noticed in the area of hilly forest with a decreasing to 51.2% in 2014.

According to the Figure 8, a substantial diminution in the hilly forest has been observed by 8.5% (832.8 sq.km.) from 1989 to 2000 and 24.85% (2229.25 sq.km.) from 2000 to 2014 with total gains were 13.82 sq.km and 492.66 sq.km respectively (Figure 8). Thus, the net change in hilly forest over the last 25 (1989 to 2014) years shown a decrease of 3062.05 sq.km.

### 3.1.2. Shrub land

Shrub land is the second dominant LULC class in the study area covering almost one-third of the total area in 2014. It increased significantly from 2173.39 sq.km (in 1989) to 2745.05 sq.km (in 2000) and the upward trend continued and substantially increased up to 5164.21 sq. km. in 2014 which was 39.2 % of the total area in 2014. At a glance, Shrub land increased by 137.61% from 1989 to 2014 study year with net increase 2990.82 sq.km area.

### 3.1.3. Crop land

This category occupies the 3rd areal position in the study area which increased by 268.73 sq.km from 1889 to 2000 with a slight decrease in 10.00 sq.km from 2000 to 2014. Over the last 25 years it gained 406.23 sq.km (Figure 8). from other categories while lost 147.49 sq.km. By this period the net change shown an increase of 258.74sq.km area.

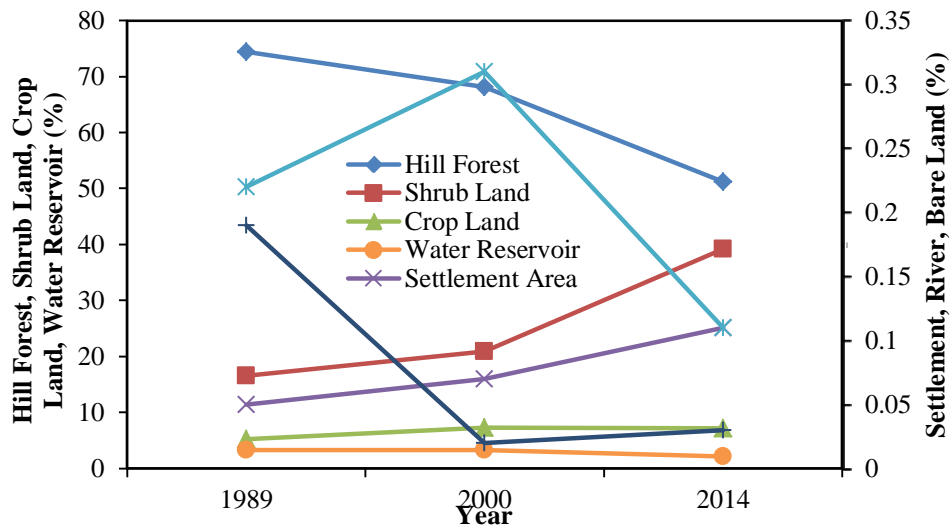


Figure 7: Area (%) of LULC categories in different study year.

### 3.1.4. River and inland water reservoir

In the year between 1989 and 2000 area under river and inland water body (water reservoir) has increased while during 2000 to 2014 those areas decreased substantially. River that increased 12.09 sq.km from 1989 to 2000, reduced considerably to 15.09 sq.km in 2014 that was 0.11 % of the total area only. There has been a slight increase in the inland water reservoir, increased only 0.77 sq.km from 1989 to 2000 but decreased up to 160.22 sq.km during the time period 2000 to 2014 which is the maximum change in this category. While investigating the net areal change both categories has shown a decreasing scenario where water reservoir decreased dramatically by 159.45sq.km during 1989 to 2014.

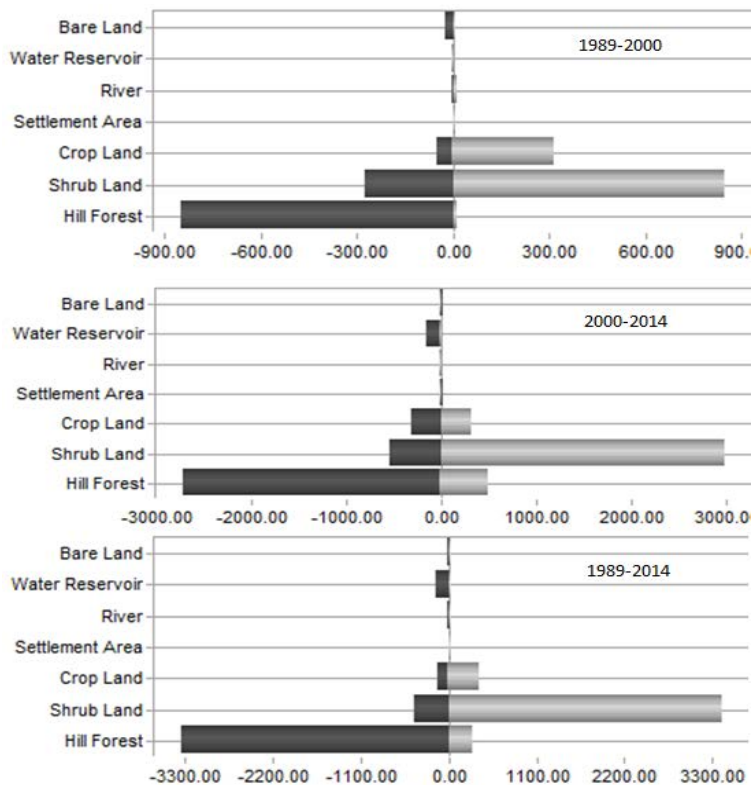


Figure 8. Gain and loss of LULC by category in different time periods. Dark and light colors are indication of loss and gain respectively.

### **3.1.5. Settlement and Bare land**

A slight increase in Human settlement (2.07 sq.km.) has been observed from 1989 to 2000 which dramatically rose up to 14.44 sq.km in 2014. On the other hand, during the 1889 to 2000 time span the region has experienced a dramatic decrease in Bare land from 25.4 sq.km to 2.87 sq.km (decreasing rate 2.05 per year) with negligible increase from 2000 to 2014 (0.07 per year). Consequently, the net increase in settlement was 7.32 sq.km. whilst net decrease in bare land was 21.54 sq.km. during 1989 to 2014.

In total, for the last 25 years, decreasing rates of Hilly forest is 122.48 per year, while increasing rate for Shrub land and Crop land is 119.63 and 10.35 per year respectively. It is worth monitoring that Hilly forest has been cut down and designing its area to Shrub land and Crop land due to shifting cultivation, feeding in brick kiln and black market as mentioned in many published documents. Over the years between 1989 and 2014, net change in Bare land, Water reservoir and River indicate that these uses have been reducing their spatial extension converting to other category especially to shrub land and crop land.

### **3.2. Change analysis**

The total transition from the period 1989 to 2014 is more or less dynamic. During the last 25 years hilly forest declined 3062.05 sq.km with a rate of 122.48 sq.km. per year which was really a terrible finding. The change area table (Table 4) revealed that between the years 1989 and 2000 hilly forest contributed 67.2% (808.54 sq.km) to shrub land and 2.9 % (35.97 sq.km) to crop land which were significantly increased to 2695.87 sq.km and 24.56 sq.km respectively by 2000-2014 study period. The total transition from the Hilly forest to shrub land and crop land over the last 25 years were 3288.75 sq.km (131.55 sq.km. per year) and 56.24 sq.km (2.25 sq.km. per year) respectively. On the contrary, hilly forest undertook 224.80 sq.km area from shrub land and 48.25 sq.km area from crop land during 1989-2014.

The result shown a significant increase in crop land mainly resulted from shrub land which is 21.5% (259.08 sq.km) during 1989-2000 and 3.38% (128.26sq. km) during 2000-2014. The increment of crop land also resulted from the water reservoir and bare land. 127.34 sq.km. (3.42%) of water reservoir and 21.06 sq.km. (0.510%) of bare land converted to crop land during 1989-2014. During this time frame crop land achieved its maximum area (overall 188.743 sq.km) from shrub land. On the contrary, it also lost its 4.79 sq.km. and 65.98 sq.km area to hilly forest in 1989-2000 and 2000-2014 respectively. The overall increment of crop land was 258.74 sq.km. in the last 25 years. Shrub land, which was occupying 16.5% of the total area in 1989 underwent the greatest growth by 2695.87 sq.km. (71.1%) from hilly forest and 237.07 sq.km. from crop land during 2000-2014 time span. The total loss of bare land between 1989 and 2014 is 21.52 sq.km, with a declining rate 0.86 per year, which was converted mostly to crop land (21.061 sq.km) and a little (1.880 sq.km) to shrub land respectively. But area under the settlement category shown steady growth while areal expansion is noticed almost double from 0.05% (7.01sq.km) to 0.11% (14.44 sq.km) during 1989-2014 which was mostly gained its area from crop land. On the other hand, the river increased 28.41 sq.km. to 40.5 sq.km. from 1989 to 2000 but reduced markedly (25.41 sq.km.) from 2000 to 2014 with conversion mainly to crop land (12.82 sq.km) and shrub land (3.91sq.km) from 1989 to 2014 at a glance (Figure 9).



### 3.3. Predicted result

Using the combined Markov and Cellular Automata future changes of LULC has been predicted for 2028 and 2042 projected years (Figure 10). The CA-Markov prediction shows a substantial loss in hilly forest areas, whereas shrub land and crop land categories shows significant growth in their aerial extension. According to the model prediction hilly forest would decrease 1191 sq.km. from 2014 to 2028 and 1831 sq.km. from 2014 to 2042 prediction periods (Table 5). In contrary, shrub land and crop land may reflect a dramatic step-up in their areas.

**Table 5:** CA-Markov predicted results and change analysis by category.

LULC Category	2028 (sq. km.)	2042 (sq. km.)	Change (sq.km.)	Change (sq.km.)
	(Simulated)	(Simulated)	(2014-2028)	(2014-2042)
Hilly forest	5549.31	4909.49	-1191.37	-1831.19
Shrub land	6411.4	7053.03	1247.19	1888.82
Crop land	994.08	1043.04	42.08	91.04
Settlement Area	16.41	21.96	1.97	7.52
River	8.14	6.59	-6.95	-8.5
Water Reservoir	186.21	131.5	-93.43	-148.14
Bare Land	3.73	3.67	-0.15	-0.21

From 2014 to 2028 shrub land would increase to 1247 sq.km. area and at the same time span crop land would gain 42 sq.km area respectively. The settlement would increase very slightly from 2014 to 2028 but it may raise to 5.5 sq.km. during the next 14 years (from 2028 to 2042). It could be the result of gradual increasing of population in the area. Other three categories (river, water reservoir and bare land) would show negative figures in the following predicted years. They may decrease to 8.5, 148 and 0.2 sq.km. areas respectively from 2014 to 2042 simulated period. Major change in forest cover and shrub land denotes the exchange of area between these two categories.

According to the previous result (Table 4) hilly forest has been contributing to the shrub land and thus playing a significant role in the expansion of the shrub land category. On the other hand, crop land has continuously been taking place of inland water bodies that may be happening due to the lowering of water level.

However, to obtain better result from the simulation of LULC, it always requires to consider other factors like socioeconomic, physical, existing policy and so on [21, 25]. The perfection also depends on the accuracy of the existing maps based on which simulation is being performed [47]. In this research, we overlooked those factors due to lacking of data. So, to achieve higher accuracy from simulation process it is highly required to the involvement of relevant factors. Finally, it may be recommended to conduct further study involving the meteorological and land surface temperature data to observe and analyze how LULC changes shaping or altering the climate of the hilly environment.

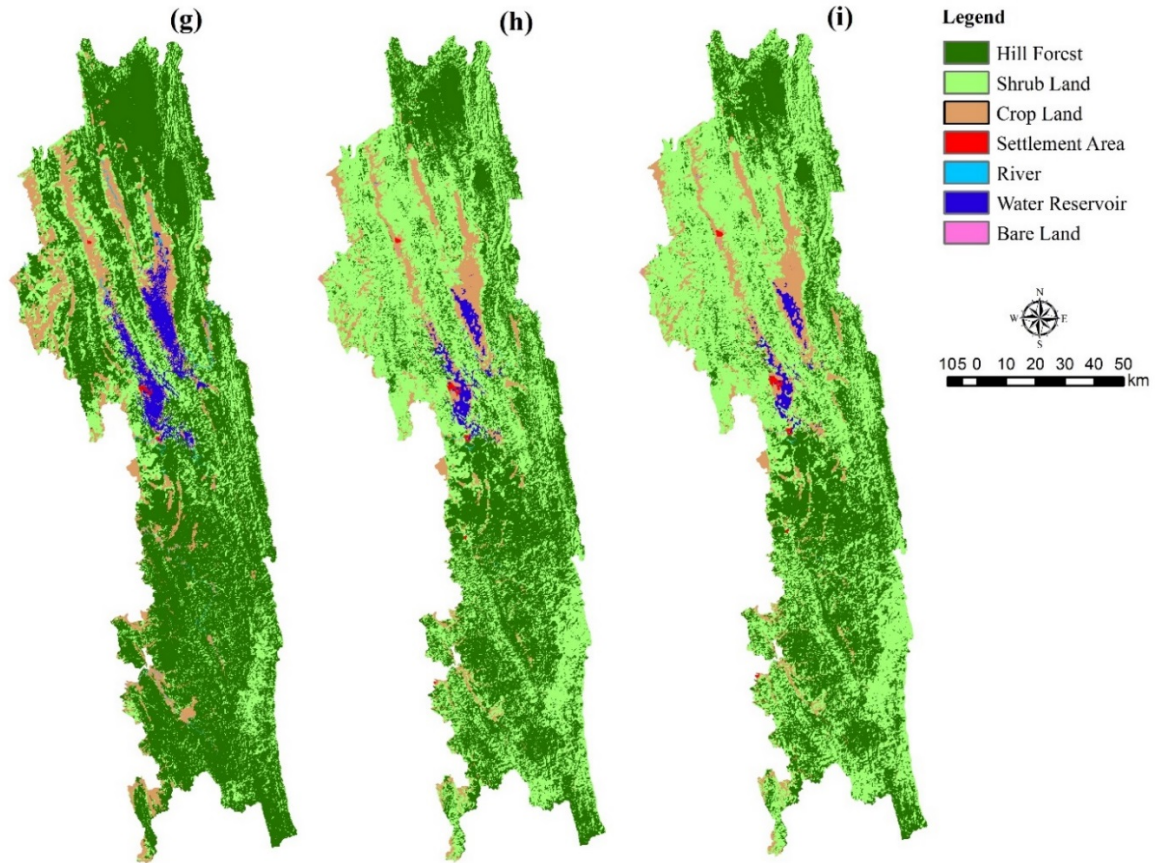


**Figure 10:** Predicted LULC maps. (g) 2014; (h) 2028; (i) 2042.

#### 4. Limitation of the research

Due to the existence of high hills and dense forest along the extreme eastern border of the study area, it was not possible to collect ground data properly. Besides, there are some reserved forest area where entry had been restricted. Unavailable transport system in some areas was another constraint in the collection of ground data. In the integrated Markov Chain and CA-Markov simulation process, some important parameters like socioeconomic, physical and existing policy were excluded due to the lacking of data. Another big limitation of this study was the use of medium resolution satellite imagery (Landsat) due to the limitation of available funds.

#### 5. Conclusion

Dynamics of land use/ land cover changes and their future scenario in the tertiary southeastern hill tracts of Bangladesh has been carried out in this paper using geospatial technology. Multi-temporal Landsat imagery on 1989, 2000 and 2014 were used to derive LULC maps which were further used in the CA-Markov process to successfully simulate the future spatial and temporal changes of LULC. Due to the rapid population growth and so called socioeconomic development the LULC has been changing constantly which could have a significant negative impact on the local hilly climate and environment.

This study reveals a substantial declining of hilly forest and along with it a continuous increasing of the shrub land area. From a careful investigation, it was found that the major conversion of hilly forest and shrub land has been taken place between each other. The results disclosed that the hilly forest has been converted to the shrub land at 131sq. km. per year approximately although in some places shrub land also converted to forest cover which was primarily due to commercial plantation by various development projects from both government and non-government agencies.

Built up area has also been extended from 7 sq. km. in 1989 to 14.44 sq.km. in 2014, with a net increase of 7.43 sq.km. over the last 25 years. Another dramatic decrease in water reservoir may cause a devastating water crisis for irrigation in the future. However, the rapid population growth, increasing demands of woods for housing, intensive pressure of land grabbers along with unplanned urban expansion are generally thought to be the prevailing dominant causes of the land use/cover changes in the hilly area of the country.

After 2001 human interference has been limited to some of forested areas by declaring them as protected area or reserved forest with a view to maintain the standard area of forest cover and to preserve a number of threatened wild species inhabiting in the area marked in IUCN Red List Books-2000. This research could provide a preliminary guideline and baseline information for sound resource management strategy in the hilly environment through sustainable land use planning and policy guidelines.

### **Acknowledgement**

We are especially grateful to BBS for providing us important census data which played vital role in the analysis. We are also grateful to the local community who helped us in every footprint of our field investigation.

### **References**

- [1] R. Anderson, E. Hardy, J. Roach and R. Witmer, "A land use and land cover classification system for use with remote sensor data, Sioux Falls, USA." *USGS professional paper*, vol. 964, 1976.
- [2] Asian Development Bank (ADB), "Chittagong Hill Tracts region development plan", Rangamati, Final Report, ADB TA No. 3328, pp. 67-103, 2001.
- [3] ATCOR, "Atmospheric/Topographic Correction of Satellite Imagery." User Guide, Version 7.1. DLR-IB 565-01/10, 2010.
- [4] Z. Bai, "Assessing land degradation in the Chittagong Hill tracts, Bangladesh, using NASA GIMMS", ISRIC – World Soil Information, Wageningen, 2006.
- [5] Bangladesh Bureau of Statistics (BBS), "Population and housing census, Community series – Rangamati, Khagrachari, Bandarban." BBS, Ministry of Planning, Dhaka, Bangladesh. 1991, 2001, 2011.

- [6] A. Berk, L. Bernstein, G. Anderson, P. Acharya, D. Robertson, J. Chetwynd and S. Adler-Golden, "MODTRAN Cloud and Multiple Scattering Upgrades with Application to AVIRIS", *Remote Sensing of Environment*, vol. 65, no. 3, pp. 367-375, 1998.
- [7] Y. Bishop, S. Fienberg and P. Holland, *Discrete multivariate analysis*. Cambridge, Mass.: MIT Press, 1975.
- [8] A. Biswas, M. Alamgir, S. Haque and K. Osman, "Study on soils under shifting cultivation and other land use categories in Chittagong Hill Tracts, Bangladesh", *Journal of Forestry Research*, vol. 23, no. 2, pp. 261-265, 2011.
- [9] D. Brown, B. Pijanowski and J. Duh, "Modeling the relationships between land use and land cover on private lands in the Upper Midwest, USA", *Journal of Environmental Management*, vol. 59, no. 4, pp. 247-263, 2000.
- [10] P. Chavez, "Image-based Atmospheric Corrections—Revisited and Improved", *Photo-grammetric Engineering and Remote Sensing*, vol. 62, no. 9, pp. 1025–1036, 1996.
- [11] P. Chavez, 1975. "Atmospheric, Solar, and M.T.F. Corrections for ERTS Digital Imagery," in *Proc., American Society of Photogrammetry*. Bethesda, MD: American Society for Photogrammetry and Remote Sensing, 1975, pp. 69–69a.
- [12] P. Chavez, G. Berlin, and L. Sowers, "Statistical method for selecting Landsat MSS ratios", *Journal of Applied Photographic Engineering*, vol. 8, no. 1, pp. 23-30, 1982.
- [13] J. Cohen, "A Coefficient of Agreement for Nominal Scales", *Educational and Psychological Measurement*, vol. 20, no. 1, pp. 37-46, 1960.
- [14] R. Congalton, and K. Green, "A practical look at the sources of confusion in error matrix generation", *Photogrammetric Engineering and Remote Sensing*, vol. 59, no. 5, pp. 641-64, 1993.
- [15] R. Congalton, "A review of assessing the accuracy of classifications of remotely sensed data", *Remote Sensing of Environment*, vol. 37, no. 1, pp. 35-46, 1991.
- [16] R. Congalton and R. Mead, "A quantitative method to test for consistency and correctness in photo-interpretation", *Photogrammetric Engineering and Remote Sensing*, vol. 49, no. 1, pp. 69-74, 1983
- [17] G. de Koning, P. Benítez, F. Muñoz and R. Olschewski, "Modelling the impacts of payments for biodiversity conservation on regional land-use patterns", *Landscape and Urban Planning*, vol. 83, no. 4, pp. 255-267, 2007.
- [18] R. Dixon, A. Solomon, S. Brown, R. Houghton, M. Trexier and J. Wisniewski, "Carbon Pools and Flux of Global Forest Ecosystems", *Science*, vol. 263, no. 5144, pp. 185-190, 1994.

- [19] A. Gafur, "Effects of shifting cultivation on soil properties, erosion, nutrient depletion and hydro-logical responses in small watershed of the Chittagong Hill Tracts of Bangladesh", Unpublished doctoral dissertation, The Royal Veterinary and Agricultural University, Copenhagen, Denmark, 2001.
- [20] M. Gilabert, C. Conese and F. Maselli, "An atmospheric correction method for the automatic retrieval of surface reflectances from TM images", *International Journal of Remote Sensing*, vol. 15, no. 10, pp. 2065-2086, 1994.
- [21] D. Guan, H. Li, T. Inohae, W. Su, T. Nagaie and K. Hokao, "Modeling urban land use change by the integration of cellular automaton and Markov model", *Ecological Modelling*, vol. 222, no. 20-22, pp. 3761-3772, 2011.
- [22] H. Tran, D. Uchihama, S. Ochi and Y. Yasuoka, "Assessment with satellite data of the urban heat island effects in Asian mega cities", *International Journal of Applied Earth Observation and Geoinformation*, vol. 8, no. 1, pp. 34-48, 2006.
- [23] K. Islam and R. Weil, "Land use effects on soil quality in a tropical forest ecosystem of Bangladesh", *Agriculture, Ecosystems & Environment*, vol. 79, no. 1, pp. 9-16, 2000.
- [24] J. Jensen, *Introductory digital image processing: A remote sensing perspective*, 3rd ed. Upper Saddle River, N.J.: Prentice Hall, 2005.
- [25] C. Kamusoko, M. Aniya, B. Adi and M. Manjoro, "Rural sustainability under threat in Zimbabwe – Simulation of future land use/cover changes in the Bindura district based on the Markov-cellular automata model", *Applied Geography*, vol. 29, no. 3, pp. 435-447, 2009.
- [26] H. Lachowski, *Guidelines for the Use of Digital Imagery for Vegetation Mapping. United States Department of Agriculture, Forest Service*. Engineering staff, Washington DC., 1995.
- [27] J. Richards, H. Skånes, W. Steffen, G. Stone, U. Svedin, T. Veldkamp, C. Vogel and J. Xu, "The causes of land-use and land-cover change: moving beyond the myths", *Global Environmental Change*, vol. 11, no. 4, pp. 261-269, 2001.
- [28] T. Lillesand and R. Kiefer, *Remote sensing and image interpretation*. New York: Wiley, 1999.
- [29] T. Lillesand, R. Kiefer and J. Chipman, *Remote Sensing and Image Interpretation*, 5<sup>th</sup> ed. Hoboken, N.J.: John Wiley and sons, 2004.
- [30] T. Loveland, Z. Zhu, D. Ohlen, J. Brown, B. Reed and L. Yang, "An analysis of IGBP global land-cover characterization process", *Photogrammetric Engineering and Remote Sensing*, vol. 65, no. 9, pp. 1021-1032, 1999.

- [31] D. Lu, E. Moran, S. Hetrick and G. Li, "Land-use and land-cover change detection", in *Advances in environmental remote sensing: sensors, algorithms and applications*, Q. Weng, Ed. Boca Raton: CRC Press, 2011, pp. 273–291.
- [32] V. Mesev, *Integration of GIS and remote sensing*. Chichester, West Sussex: Wiley, 2007.
- [33] M. Muller and J. Middleton, "A Markov model of land-use change dynamics in the Niagara region, Ontario, Canada", *Landscape Ecology*, vol. 9, pp. 151-157, 1994.
- [34] A. Nishat and S. Biswas, "Community-based restoration of degraded tropical hill forests: Experiences from Krykhong Para, Chittagong Hill Tracts, Bangladesh", *National Institute of Ecology, Jaypur/New Delhi*, no. 16, pp. 1-11, 2005.
- [35] G. Pontius and J. Malanson, "Comparison of the structure and accuracy of two land change models", *International Journal of Geographical Information Science*, vol. 19, no. 2, pp. 243-265, 2005.
- [36] F. Quéfier, S. Lavorel, W. Thuiller and I. Davies, "PLANT-TRAIT-BASED MODELING ASSESSMENT OF ECOSYSTEM-SERVICE SENSITIVITY TO LAND-USE CHANGE", *Ecological Applications*, vol. 17, no. 8, pp. 2377-2386, 2007.
- [37] G. Rasul, G. Thapa and M. Zoebisch, "Determinants of land-use changes in the Chittagong Hill Tracts of Bangladesh", *Applied Geography*, vol. 24, no. 3, pp. 217-240, 2004.
- [38] G. Rasul, "Political ecology of the degradation of forest commons in the Chittagong Hill Tracts of Bangladesh", *Envir. Conserv.*, vol. 34, no. 02, p. 153, 2007.
- [39] J. Rouse, R. Haas, J. Schell, and D. Deering, "Monitoring vegetation systems in the Great Plains with ERTS", Third ERTS Symposium, Technical Presentation NASA SP-351, vol. I, pp. 309-317, 1973.
- [40] R. Roy, "Land forest rights in the Chittagong Hill Tracts, Bangladesh", International Centre for Integrated Mountain Development (ICIMOD), Kathmandu, Nepal, 2002.
- [41] L. Sang, C. Zhang, J. Yang, D. Zhu and W. Yun, "Simulation of land use spatial pattern of towns and villages based on CA–Markov model", *Mathematical and Computer Modelling*, vol. 54, no. 3-4, pp. 938-943, 2011.
- [42] K. Seto and R. Kaufmann, "Modeling the Drivers of Urban Land Use Change in the Pearl River Delta, China: Integrating Remote Sensing with Socioeconomic Data", *Land Economics*, vol. 79, no. 1, p. 106-121, 2003.
- [43] M. Tolba, O. El-Kholy and E. El-Hinnawi, *The world environment 1972-1992 ; two decades of challenge*. London: Chapman and Hall, 1992.

- [44] Q. Weng, D. Lu and J. Schubring, "Estimation of land surface temperature–vegetation abundance relationship for urban heat island studies", *Remote Sensing of Environment*, vol. 89, no. 4, pp. 467-483, 2004.
- [45] G. Xian, M. Crane and J. Su, "An analysis of urban development and its environmental impact on the Tampa Bay watershed", *Journal of Environmental Management*, vol. 85, no. 4, pp. 965-976, 2007.
- [46] Y. Yamaura, T. Amano, T. Koizumi, Y. Mitsuda, H. Taki and K. Okabe, "Does land-use change affect biodiversity dynamics at a macroecological scale? A case study of birds over the past 20 years in Japan", *Animal Conservation*, vol. 12, no. 2, pp. 110-119, 2009.
- [47] F. Yuan, "Urban growth monitoring and projection using remote sensing and geographic information systems: a case study in the Twin Cities Metropolitan Area, Minnesota", *Geocarto International*, vol. 25, no. 3, pp. 213-230, 2010.